Biomedical Signal Processing and Control 80 (2023) 104268

Contents lists available at ScienceDirect

Biomedical Signal Processing and Control

journal homepage: www.elsevier.com/locate/bspc

Deep learning models-based CT-scan image classification for automated screening of COVID-19

Kapil Gupta *, Varun Bajaj

Electronics and Communication Discipline, PDPM Indian Institute of Information Technology Design and Manufacturing, Jabalpur, MP, 482005, India

ARTICLE INFO

Keywords:
COVID-19
Deep learning
CT-scan images
Transfer learning

ABSTRACT

COVID-19 is the most transmissible disease, caused by the SARS-CoV-2 virus that severely infects the lungs and the upper respiratory tract of the human body. This virus badly affected the lives and wellness of millions of people worldwide and spread widely. Early diagnosis, timely treatment, and proper confinement of the infected patients are some possible ways to control the spreading of coronavirus. Computed tomography (CT) scanning has proven useful in diagnosing several respiratory lung problems, including COVID-19 infections. Automated detection of COVID-19 using chest CT-scan images may reduce the clinician's load and save the lives of thousands of people. This study proposes a robust framework for the automated screening of COVID-19 using chest CT-scan images and deep learning-based techniques. In this work, a publically accessible CT-scan image dataset (contains the 1252 COVID-19 and 1230 non-COVID chest CT images), two pre-trained deep learning models (DLMs) namely, MobileNetV2 and DarkNet19, and a newly-designed lightweight DLM, are utilized for the automated screening of COVID-19. A repeated ten-fold holdout validation method is utilized for the training, validation, and testing of DLMs. The highest classification accuracy of 98.91% is achieved using transfer-learned DarkNet19. The proposed framework is ready to be tested with more CT images. The simulation results with the publicly available COVID-19 CT scan image dataset are included to show the effectiveness of the presented study.

1. Introduction

Coronaviruses are a vast group of viruses that may induce a variety of infections ranging from the common cold and cough to serious respiratory problems. The majority of coronaviruses are not very harmful. SARS-CoV-2 is a new variant of coronavirus that has never been detected earlier in humans [1]. This virus was found at the end of 2019 in the Wuhan province of China and critically affects the lungs of an infected person [2]. COVID-19 is the most transmissible disease caused by the SARS-CoV-2 virus [3]. COVID-19 is the name given to this new strain by the World health organization (WHO), which causes millions of fatalities worldwide. The majority of people affected by COVID-19 are suffering from mild to medium respiratory problems and recover without any specific treatment. However, some patients are severely suffering from respiratory problems and require specific medical assistance [4]. Serious infection is more likely to strike people over the age of 55, as well as those who had been earlier diagnosed with some medical illnesses such as diabetes, hypertension, chronic respiratory disease, cardiac abnormalities, or cancer [5]. Since March 2020, the COVID-19 virus has spread aggressively with incompletely unresolved transmission procedures and has become a worldwide pandemic with the number of cases and mortality continuing to rise on a daily basis [6]. Moreover, in several countries, along with the United States, animals like cats and dogs are also infected with SARS-CoV-2. In March 2020, WHO decided to declare this a "Public health emergency of international concern" [7]. Real-time reverse transcription-polymerase chain reaction (RT-PCR) testing is commonly used by front-line health workers or clinicians to diagnose COVID-19 infections [8]. RT-PCR test is a molecular test that specifically targets a particular section of the ribonucleic acid (RNA) of the virus that could not be present in other subfamilies [9]. RT-PCR testing is currently one of the most widely used methods for screening COVID-19 infections, but it is a painful, time-taking, and complex process. Some previous research showed its low sensitivity (below 70%) in the early stages [10]. To perform RT-PCR testing, healthcare workers are required to come in contact with patients, which can also increase the risk of infection with the coronavirus [11]. There are several other problems with using RT-PCR, such as a shortage of suitable test kits, expenses, hazards to the safety of health workers, and a long wait time for test results [12]. To address these limitations and the availability and accessibility of commercial examinations, several different diagnostic approaches were

* Corresponding author.
E-mail address: 20peco06@iiitdmj.ac.in (K. Gupta).

https://doi.org/10.1016/j.bspc.2022.104268
Received 8 July 2022; Received in revised form 7 September 2022; Accepted 26 September 2022
Available online 30 September 2022

investigated, particularly when RT-PCR is not available or the test reports are delayed [13]. Chest computed tomography scanning (CT-scan) is one of them, that has been proven to be beneficial in monitoring the effects of COVID-19 on lung tissue [6]. Chest CT scanning provides a precise image of blood arteries, organs, soft tissues, and bones. CT scans provide a much more extensive picture of the patient's health that helps clinicians to detect internal structures and assess their size, shape, texture, and density [14]. Manual scanning of COVID-19 using chest CT scans is tedious, time-taking, and subject to human mistakes. Also, the number of COVID-19 cases rises at an accelerating rate [15]. Therefore, an automated COVID-19 screening system is needed. This will aid in faster virus diagnosis at various stages, relieving healthcare workers from the tedious process of manual annotation [3]. Consequently, researchers have presented a variety of approaches for the automated screening of COVID-19 using different scanning techniques, which are summarized in the next section. The remainder of this article is structured as follows: Section 2 provides the previous work; the proposed method is presented in Section 3; experimental setup and findings are depicted in Section 4; discussion of this work with previous works on the same CT-scan data is depicted in Section 5; conclusion of this work is drawn in Section 6.

2. Previous work

Nowadays, various artificial intelligence-based techniques are widely investigated in large fields from neuroscience to computer science. Deep learning models (DLMs) can be used in both 1-dimensional single-channel, 1-D multi-channel, and 2-D (images) data analysis. In [16], the author proposed an emotional complexity marker for classifying different emotions induced by affective video film clips. They classified nine different emotional states using DLM and reported the highest classification accuracy. In [17], the Support Vector Machines (SVMs) classifier has been utilized to classify discrete emotional states. In another study [18], authors proposed a machine learning model for the classification of various cognitive and behavioral emotion regulation strategies. The deep learning-based technique also has the potential to diagnose different cardiovascular diseases. For example, Gupta et al. [19] proposed a novel DLM for the screening of bundle branch blocks using vectorcardiogram signals. In [20], authors proposed a new deep learning framework namely Hyp-Net for the automated detection of hypertension using time-frequency images of 1-D ballistocardiogram signals. Sometimes, for the better classification of medical images, authors compute the features like moments from the images. For this reason, authors [21] proposed a new set of polar harmonic Fourier moments and invariant continuous orthogonal moments. Wang et al. [22] presented continuous orthogonal moments using Trinion Fractional-Order. Medical image protection without degrading the quality of original images is also a challenging task. A color medical image watermarking scheme has been proposed by Xia et al. [23]. By motivating from the facts described above, researchers have explored a variety of automated detection systems for screening COVID-19 using different scanning methods. Various DLMs with decision fusion techniques have been utilized to diagnose COVID-19 infected persons using CT-scan images by Mishra et al. [24]. In [25] a new DLM has been presented to identify COVID-19 patents. Pre-trained DenseNet201 has been employed to classify COVID-19 infected patients by Jaiswal et al. [26]. Wang et al. [27] presented a novel deep convolutional-based method for the screening of coronavirus disease. In [28] authors utilized a pre-trained DensNet-121 to detect COVID-19 patients using CT-scans. Benchmark DenseNet121 has been used to classify COVID-19 subjects by Sarkar et al. [29]. They utilized the transfer learning method for model training. Gaur et al. [30] utilized 2D-empirical wavelet transformation (EWT) technique to select the best performing channel. They detected COVID patients by classifying wavelet sub-bands using the benchmark DenseNet121 model. Classifier fusion method has been employed to detect COVID-19 by Kaur et al. [3]. They explored different variants of ResNet architecture and used transfer learning techniques to build the model. eXplainable deep network has been proposed to categorize COVID and non-COVID data by Soares et al. [31]. A whale optimization algorithm has been employed to optimize the hyper-parameters of a generative adversarial network (GAN) by Goel et al. [32]. They proposed an optimized GAN for automatic screening of COVID-19. Deep learning based COVID-19 detection system has been proposed by Lu et al. [33]. Basu et al. [34] utilized three different pre-trained DLMs (DenseNet, ResNet, and XceptionNet) to extract the deep features from CT scan images. A combination of local search techniques with optimization algorithms has been employed for feature selection. They fed selected features into dense layers and classify normal and COVID patients.

In the existing literature, the majority of COVID-19 screening methods have chosen to manually select tuning boundaries for the effective decomposition of physiological data. This human selection of parameters could lead to mode mixing, time-frequency trade-off, and band restrictions of the filter bank could result in information loss. Furthermore, the classification performance of the presented techniques/methods in the literature is limited in the form of accuracy. Therefore, a more reliable framework is presented in this study for the accurate detection of COVID-19 using chest CT scans. In this work, two pre-trained DLMs namely, MobileNetV2 [35] and DarkNet19 [36] are utilized for the automated and accurate screening of COVID-19. Transfer learning is applied to re-train the benchmark DarkNet19 and MobileNetV2. A novel less complex DLM is also proposed in this study for the classification of chest CT images. To match the input image size of the employed DLMs, all images are resized to 224×224 for MobileNetV2, 227×227 for newly developed DLM, and 256×256 for DarkNet19. The vital contributions of this work are as follows:

1. A new lightweight, less complex DLM is developed for the automated screening of COVID-19 using chest CT scans. A comparative experimental study is also performed with two different networks namely, Dark-Net19 and MobileNetv2 with a transfer learning strategy.
2. DLMs are trained using a repeated 10-fold holdout cross-validation (10-FHCV) scheme.

3. Proposed method

In the proposed method, a DLM-based technique is utilized to detect COVID-19 infected subjects using chest CT-scan images. Collected chest CT-scan images are resized as per the requirement of utilized DLMs. This approach uses a transfer learning technique to re-train the benchmark DarkNet19 and MobileNetV2. A newly designed less complex, lightweight DLM has also been employed to classify the chest CT images into COVID and non-COVID classes. A repeated 10-FHCV scheme is used to develop a robust framework. Eight performance characteristics are evaluated to check the efficiency of the developed framework. The layered architecture of the proposed methodology is depicted in Fig. 1. A brief description of DLM, transfer learning techniques, repeated 10-FHCV schemes, and performance metrics are given in the subsequent subsections.

3.1. Deep learning model

Deep-learning methodologies, such as deep feature extraction, fine-tuning of benchmarked DLM by transfer learning, and end-to-end training of a newly developed DLM are employed to identify COVID-19 and healthy (non-COVID) chest CT images. The DLM is one of the most powerful neural networks in use today, with several tasks in pattern recognition applications, including image classification, segmentation, object location, and detection. It has also proven its effectiveness in the biomedical field for signal classification and disease detection, image classification, and segmentation problems, particularly in lung

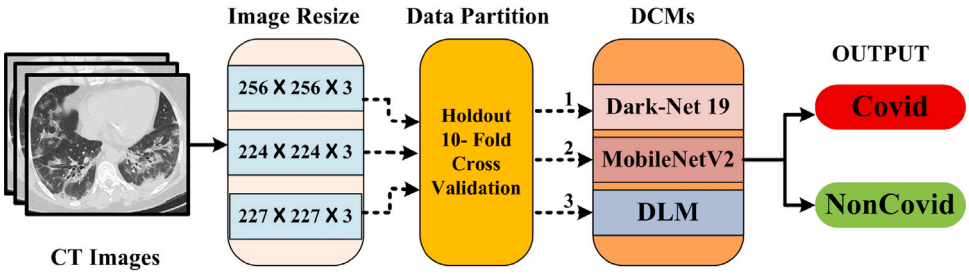

Fig. 1. Layered architecture of the presented methodology.

disorders such as lung nodule identification, pneumonia detection, and pulmonary TB detection [37]. DLMs are based on a representation-based learning system, in which a DLM automatically learns a variety of useful feature representations and combines feature extraction and classification steps into a single pipeline that can be trained from start to end without the need for manual setup or expert human involvement [38]. The DLM mainly consists of an input layer, one to many convolutional 2-D layers (Conv2DL), pooling layers (PL), and some fully connected layers (FCL). The functioning of each layer is given as follows:

1. *Conv2DL:* It consists of 2D kernels (filters) that move over the input image. A 2-D filter is a $n \times n$ dimension matrix that will be convolved with the input images, and the stride specifies how much the kernel will convolve over the input image. A stride (s) of one is frequently chosen, and a stride greater than one is used to downsample the feature maps. The 2-D convolutional operation can be defined as,

$$W[i,j] = \sum_{p=-\infty}^{\infty} \sum_{q=-\infty}^{\infty} U[p,q]V[i-p, j-q] \tag{1}$$

where V is the input image matrix to be convolved with the kernel matrix U to produce a new matrix W representing the output image. The indices i and j deal with image matrices, while p and q deal with kernel matrices. The 2-D convolutional output is also termed the output feature map. Sometimes, padding of zeros of size (P) is also employed with the output feature maps to maintain the size. For an input chest CT scan image of width X_{in}, height Y_{in} with C_{in} number of channels, and the output image width X_{op} and height Y_{op} with filters of size $n * n$ can be given as [39],

$$\begin{aligned} X_{op} &= \left[\frac{X_{in} - n + 2P}{s}\right] + 1, \\ Y_{op} &= \left[\frac{Y_{in} - n + 2P}{s}\right] + 1 \end{aligned} \tag{2}$$

An activation function is a mathematical procedure that maps an output to a sequence of inputs. They are used to make the network structure non-linear. The rectifier linear unit (ReLU) is a well-known deep learning activation function. It is given as,

$$R(X) = max(0, X) \tag{3}$$

In this work, ReLU is used after each Conv2DL.

2. *PL:* This layer is often referred to as the down-sampling or sub-sampling layer. To prevent overfitting and minimize computational complexity, the pooling operation decreases the number of neurons from the Conv2DL. Two types of pooling functions, the average Pooling function, and the max-pooling function are generally used to speed up calculations. The max-pooling function takes only the maximum value in each feature map, resulting in fewer output neurons. The average-pooling function takes the average value in each feature map. In this paper, the max-pooling procedure is employed [39].
3. *FCL:* Fully-connected means that each neuron in the upper layer is connected to every neuron in the next layer. FCL is a standard artificial neural network, with each input connected to each output by a learning weight. It works similarly to a standard multi-layer perceptron neural network. It transforms the 2D output feature map into 1D. The number of output classes decides the total number of fully-connected neurons in the last layer. To assign the output value from the last FCL to the desired class probability, a softmax function is utilized. Each value ranges between 0 and 1.

One may design their own DLM by combining the layers listed above. The number of Conv2DLs, PLs, and FCLs can be increased or decreased until the model achieves the required performance [40]. As a result of recent advancements in deep learning various pre-trained DLMs have been employed for different machine learning applications. Some well-known benchmarked transfer learning models are DarkNet19, MobileNetV2, AlexNet, GoogleNet, ResNet, and so on. In this work, two pre-trained DLMs, namely, DarkNet19 and MobileNetV2, and one newly proposed less complex DLM are used for COVID-19 screening using chest CT images. A brief detail of these models is given below:

3.1.1. *DarkNet19*

It is a new generation pre-trained DLM, that accepts the input image of size 256 × 256. This model is used as a backbone of YOLOv2 architecture. The model is composed of exactly 19 Conv2D layers and 5 PLs using Maxpool, with only 3 × 3 convolutional kernels used to reduce the number of trainable parameters. After each pooling stage, the number of channels is increased to two. To make predictions in the model, it employs 1 × 1 convolutional kernels to reduce the global average pooling and feature representation. The DarkNET19 performs admirably in terms of real-time object detection [36,41]. In comparison to frequently used DLMs, the model treats object detection as a straightforward regression issue. Initially, the DarkNet19 model had been trained to classify Image-Net data (contains 1000 classes). Consequently, the last three layers namely, FCL, SOFTMAX layer, and classification layer were configured for Image-Net data. The last FCL has 1000 neurons.

3.1.2. *MobileNetV2*

It is a recently developed DLM specifically designed for mobile devices, accepts the input image of size 224 × 224, and is developed by Sandler et al. [35]. A depth separable convolution unit dependent on the inverted residuals with linear bottleneck is a major component of MobileNetV2. In comparison to MobileNetV1, the key enhancement of MobileNetV2 is the integration of linear bottleneck and inverted residual units in the model. This bottleneck adds a 1 × 1 convolutional kernel next to the depthwise Conv2D layers, utilizes linear activation after the pointwise Conv2D layers instead of nonlinear activation, and accomplishes downsampling by adjusting the parameters in the depthwise convolutional layer. The MobileNetV2 had been developed to categorize Image-Net data. Therefore, the last three layers namely, FCL, SOFTMAX layer, and classification layer of MobileNetV2 model were fixed as per Image-Net data. The last FCL has 1000 neurons.

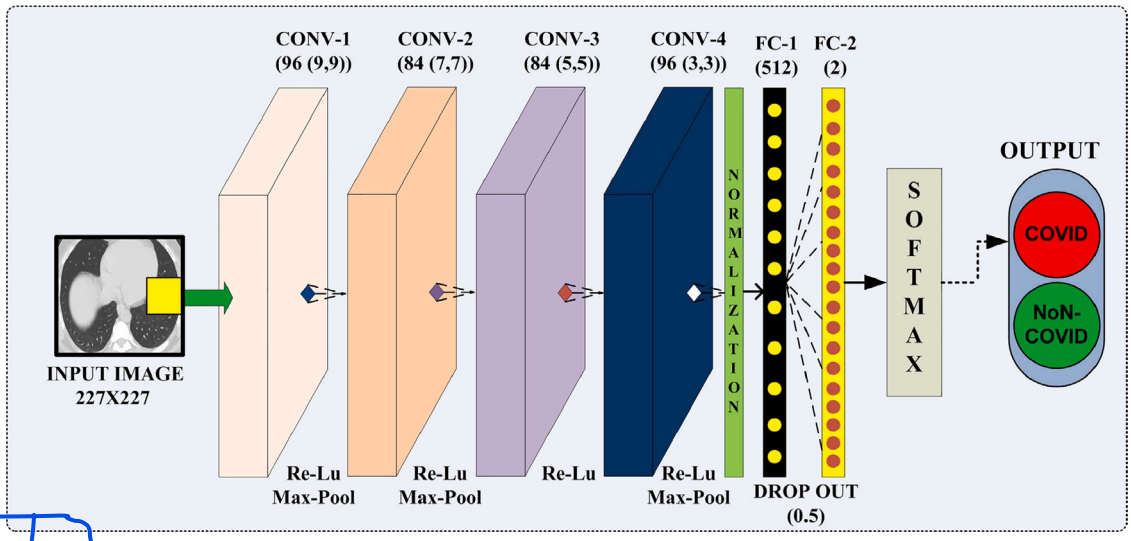

Fig. 2. Layered architecture of the developed DLM.

3.1.3. Proposed DLM

For the analysis and categorization of biomedical signals and images, there is no standard DLM available. The choice to use a DLM is based on its performance, classification accuracy, and training time. Many existing DLMs have a complex architecture and a large number of layers, that increase the number of learnable parameters. The classification accuracy of a DLM may be adjusted by changing the kernel size, stride, dropout percentage, and other parameters. The proposed DLM accepts the input image of size 227 × 227. It contains four Conv2D layers, two PLs, and two FCLs. The number of kernels used is 96, 84, 84, 96 with a kernel size of 9 × 9, 7 × 7, 5 × 5, and 3 × 3 with a stride of 2. Max pooling is utilized in PL, and 512 and 2 neurons are used in FCL with 0.5 dropouts. The layered architecture of the developed DLM is depicted in Fig. 2.

3.2. Transfer learning

A collection of a huge labeled dataset and significant hardware resources are required to train a benchmark DLM from scratch. Due to the small number of datasets, and hardware restrictions, training a benchmark model from scratch is difficult or impractical. Hence, a transfer learning approach is employed in this study to get better results. The reuse of a pre-trained DLM on a new task is referred to as transfer learning. It is an effective representation-based learning method in which pre-trained DLMs that have been trained on ImageNet data (contains records of 1000 classes with 1.2 million images), are re-utilized for a new application [42]. There are three types of transfer learning strategy namely, DLM as a fixed feature extractor, Fine-tuning the DLM, and pre-trained models. In this work, two benchmarks pre-trained DarkNet19 and MobileNetV2 are used. We have removed the last three layers of these models and used the rest of the model as a fixed feature extractor for the new COVID-19 CT-scan dataset. Fig. 3 depicts the schematic view of transfer learning.

3.3. Repeated 10-FHCV scheme

Cross-validation is a technique used to build a DLM, that splits the original input data into a training set, a validation set, and a test set for training, validation, and analyzing the model performance. In the 10-FHCV scheme, the original input data is randomly divided into 10 segments. In this work, complete chest CT data is divided into 10 equal parts, a single part is retained as the test data for DLM testing, one part of the remaining data is a holdout for validation, and the rest parts are utilized for model training [43]. A repeated 10-FHCV strategy is applied to build the DLMs. In this scheme, the cross-validation procedure is repeated 10-times by altering the training, validation, and test data. Fig. 4 depicts the schematic view of the data partition strategy.

3.4. Performance metrics

To evaluate the superiority of the presented system, eight parameters namely, accuracy (A_{CC}), sensitivity (S_{EN}), specificity (S_{PE}), F-1 score, precision (PRC), negative prediction value (N_{PV}), Fowlkes–Mallows index (F_M) and area under the curve (AUC) are used as performance metrics. The mathematical expression of these metrics is given below:

$$A_{CC}(\%) = \frac{T_{Pos} + T_{Neg}}{T_{Pos} + F_{Neg} + T_{Neg} + F_{Pos}} \times 100 \tag{4}$$

$$S_{EN}(\%) = \frac{T_{Pos}}{T_{Pos} + F_{Neg}} \times 100 \tag{5}$$

$$S_{PE}(\%) = \frac{T_{Neg}}{T_{Neg} + F_{Pos}} \times 100 \tag{6}$$

$$F-1\ score = \frac{2 \times T_{Pos}}{2 \times T_{Pos} + F_{Pos} + F_{Neg}} \tag{7}$$

$$PRC = \frac{T_{Pos}}{T_{Pos} + F_{Pos}} \tag{8}$$

$$N_{PV} = \frac{T_{Neg}}{T_{Neg} + F_{Neg}} \tag{9}$$

$$F_M = \sqrt{\frac{T_{Pos}^2}{(T_{Pos} + F_{Pos})(T_{Pos} + F_{Neg})}} \tag{10}$$

where, true positive (T_{Pos}), false positive (F_{Pos}), true negative (T_{Neg}), and false negative (F_{Neg}) are the confusion matrix parameters.

4. Experimental setup and findings

A publicly available SARS-CoV-2 chest CT-scan dataset is utilized to evaluate the performance of the proposed framework. The CT-scan images are only annotated with numbers and do not specify whether they are subject-independent or not. The CT scan image data are processed on a single CPU having a Core i7 processor, installed with 24-GB RAM, and 512-GB hard disk, in a MATLAB platform. In this work, the hyperparameters are selected based on previous studies and various experiments. Adam optimizer combines the best aspects of the AdaGrad and RMSProp algorithms and uses less memory than other

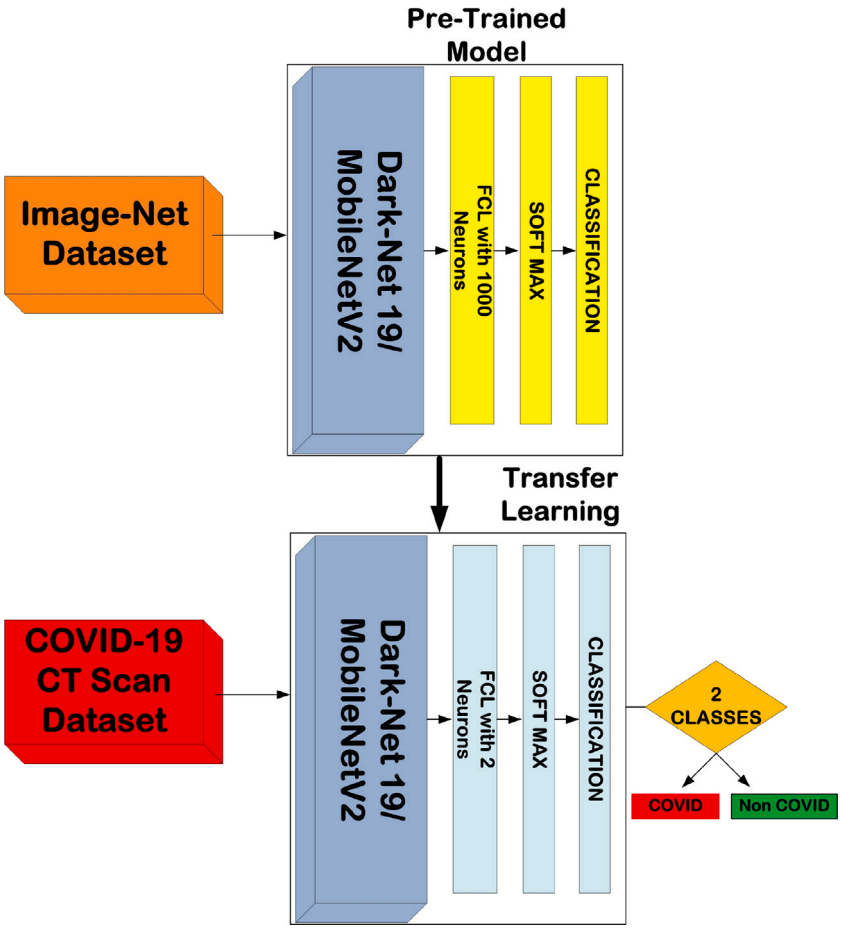

Fig. 3. Schematic view of transfer learning.

optimization techniques. Consequently, the Adam optimizer is used to optimize the cross-entropy loss. 20 epochs with a batch size of 64 and a validation frequency of 10 with an initial learning rate of 0.0001 are chosen for proper training of the DLMs. The experiment is conducted with the same setup for all three models. More details about the CT-scan dataset are given in the next subsection.

4.1. *Dataset*

For this work, the publicly accessible SARS-CoV-2 chest CT scan database [31] is utilized. The dataset was taken from non-COVID and clinically confirmed COVID-19 patients in Sao Paulo, Brazil, hospitals, and approved for research purposes by the ethical committee. This dataset contains the chest CT images of 1252 COVID-19 patients and 1230 non-COVID subjects. The identity of each subject is hidden by the hospital due to privacy issues. These CT scan images are in the .png file extension and have dimensions that vary from 182×129 to 488×408 with 32-bit depth. To match the input image size of the employed models, all images are resized to 256×256 for DarkNet19, 224×224 for MobileNetV2, and 227×227 for newly developed DLM. Fig. 5 represents six randomly selected CT-scans of (a) COVID-19 (b) non-COVID classes.

4.2. *Results*

A total of 620 iterations are required to classify COVID and non-COVID subjects. To complete training at each fold, DarkNet19 requires 238 min, MobileNetV2 requires 177 min, and proposed DLM requires only 94 min. Table 1 gives the fold-wise classification accuracy of developed DLM, MobileNetV2, and DarkNet19. The highest average classification accuracy of 98.91% is obtained for DarkNet19. Fig. 6 depicts the training and validation accuracy graphs obtained for CT scan images using: (A) DLM (B) MobileNetV2 (C) DarkNet19. It can be understood from the figure that the developed DLM required approx 200 iterations, MobileNetV2 needed around 200 iterations, and DarkNet19 required approx 180 iterations to achieve its maximum accuracy. The loss percentage and training time for the proposed model is minimum compared to pre-trained DarkNet19 and MobileNetV2. Tables 2, Table 3, and Table 4 represents the overall confusion matrix (CM) obtained for proposed DLM, MobileNetV2, and DarkNet19. Eight performance parameters are computed to better understand the proposed method for screening COVID-19. Table 5 gives the overall performance metrics obtained for proposed DLM, MobileNetV2, and DarkNet19. It is evident from Table 5 highest performance metrics are obtained by DarkNet19. The DarkNet19 outperforms the other employed DLMs because it uses several global kernels and doubles the number of channels after each pooling layer making the model efficient for object detection. Fig. 7 shows the overall receiver operating characteristic curve plots achieved for explored DLMs. The highest area is covered by DarkNet19.

5. Discussion

Rapid and correct screening of COVID-19 patients is the need of the hour. Two pre-trained DLMs along with a newly developed less complex DLM are explored in this article to classify CT-scan images for screening of COVID-19 patients. The presented technique is compared with other state-of-the-art methods. The comparison of the presented technique with previous methods for automated screening of COVID-19 using CT-scan data is depicted in Table 6. Kaur et al. [3] explored various

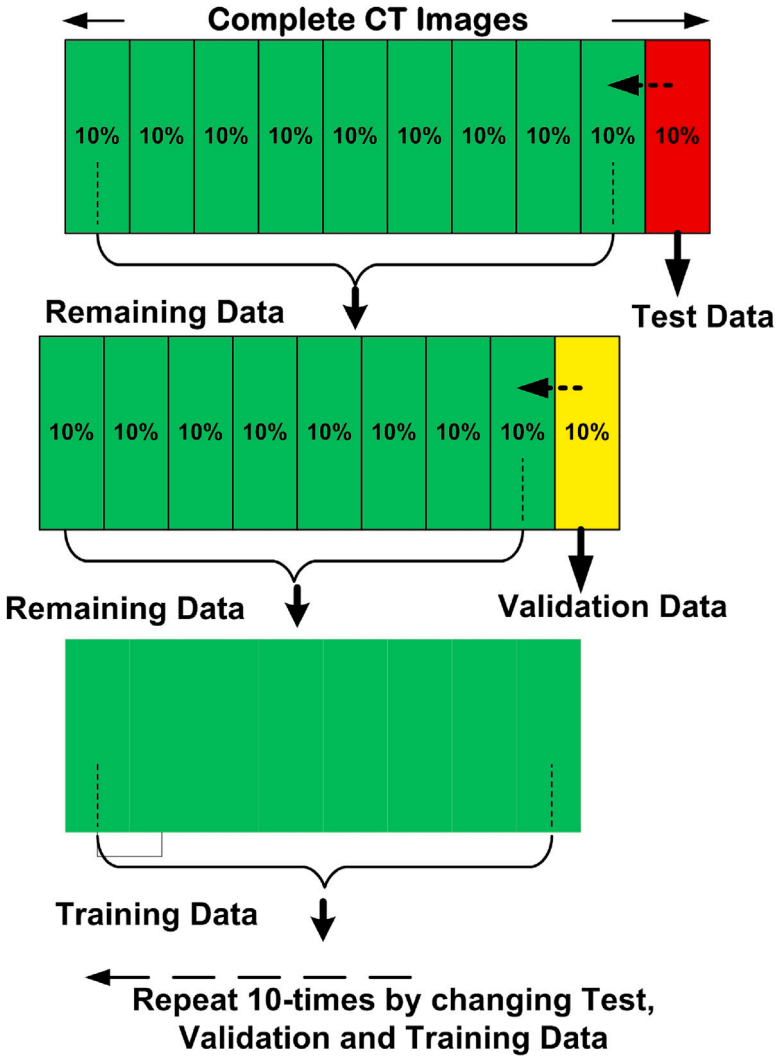

Fig. 4. Schematic view of the data partition.

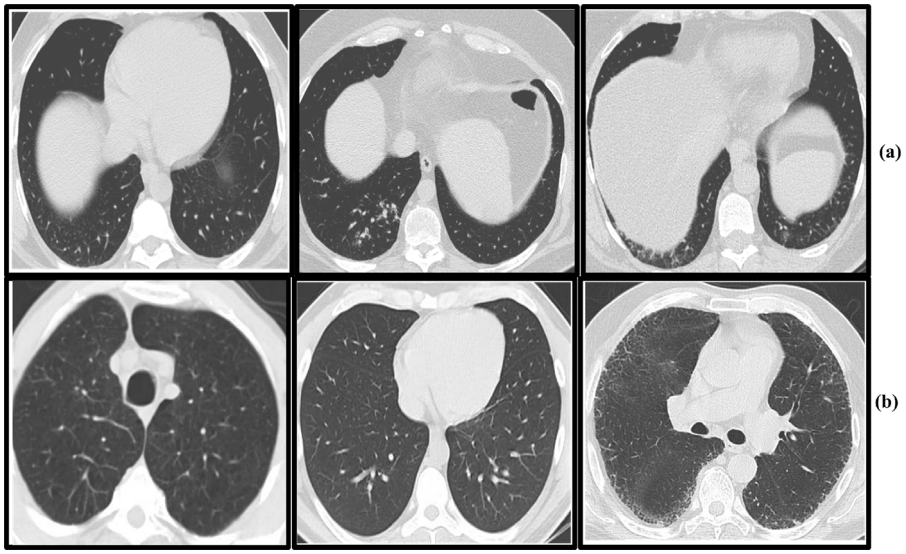

Fig. 5. Six random CT-images of (a) COVID-19 (b) Healthy classes.

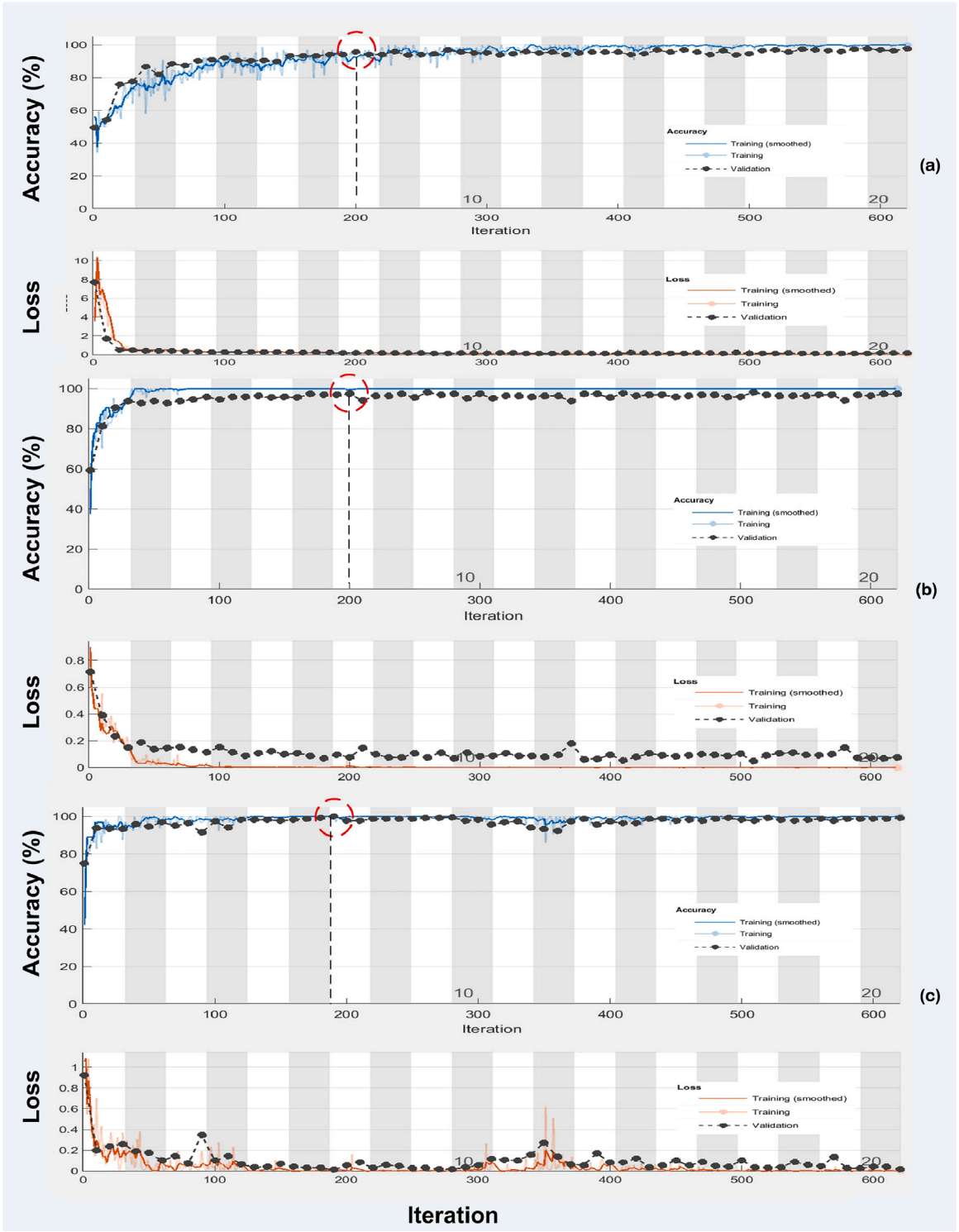

Fig. 6. Training progress graphs obtained for: (A) DLM (B) MobileNetV2 (C) DarkNet19.

DLMs and reported an ACC of 98.35%, and PRC of 98.02%, using classifier fusion with pre-trained ResNet50 model. Mishra et al. [24] also investigated different DLMs and combined the predictions of individual models by using the decision fusion technique. Their system yielded the highest classification ACC of 88.34% and $F1-score$ of 0.86 using DenseNet121. Li et al. [25] developed a new convolutional model (COVNet) using CT scan images, and reported the highest SEN of 90% and SPE of 96%. Jaiswal et al. [26] proposed DesNet201 based DLM and employed transfer learning technique for model training. Their model yielded the highest testing ACC of 96.25% and PRC of 96.29%. Wang et al. [27] modified the architecture of inception-Net using the transfer learning technique and reported an ACC of 89.5% and SEN of 87.0%. Gaur et al. [30] utilized EWT and build DenseNet121 model using transfer learning technique. Their proposed system obtained the highest classification ACC of 85.5% and $F1-score$ of 0.85. Soares et al. [31] build a DLM and reported the highest ACC of 88.6% and PRC of 89.7%. Optimized GAN proposed by Goel et al. [32] for automated screening of COVID19, obtained the highest

Table 1
Fold-wise classification accuracy of developed DLM, MobileNetV2, and DarkNet19.

Fold No.	DLM	MobileNetV2	DarkNet19
1	95.58	96.79	98.80
2	96.37	97.58	98.39
3	95.56	97.18	98.39
4	95.56	97.58	99.19
5	98.39	98.79	99.19
6	96.37	98.39	99.60
7	95.97	97.58	99.60
8	94.76	97.58	99.60
9	94.76	97.58	98.39
10	95.97	97.18	97.98
Average	95.93	97.62	**98.91**

Table 2
Overall CM obtained for proposed DLM.

		COVID	NON-COVID	
Output Class	COVID	1190	39	1229
	NON-COVID	62	1190	1252
		1252	1229	2481
		Target Class		

Table 3
Overall CM obtained for MobileNetV2.

		COVID	NON-COVID	
Output Class	COVID	1224	31	1255
	NON-COVID	28	1198	1226
		1252	1229	2481
		Target Class		

Table 4
Overall CM obtained for DarkNet19.

		COVID	NON-COVID	
Output Class	COVID	1239	14	1253
	NON-COVID	13	1215	1228
		1252	1229	2481
		Target Class		

Table 5
Overall performance metrics obtained for proposed DLM, MobileNetV2, and DarkNet19.

Parameters	DLM	MobileNetV2	DarkNet19
$A_{CC}(\%)$	95.93	97.62	98.91
$S_{EN}(\%)$	95.05	97.76	98.96
$S_{PE}(\%)$	96.82	97.47	98.86
$F1-score$	0.96	0.98	0.99
$PRC(\%)$	96.82	97.52	98.88
$N_{PV}(\%)$	95.04	97.71	98.94
F_M	0.96	0.98	0.99
$AUC(\%)$	98.94	99.67	99.89

SPE of 97.78% and $F1-score$ of 0.98. Lu et al. [33] proposed a graph theory based CGENet and reported an ACC of 97.78%. Basu et al. [34] applied feature selection technique and reported the highest ACC of 97.78% and PRC of 92.88%. In the proposed method transfer learning technique is employed for the training of pre-trained DLM Darknet19 and MobileNetV2. A less complex DLM is also proposed in this paper. A repeated 10-FHCV scheme is used to build the models. The highest classification ACC of 98.91%, PRC of 98.88%, and $F1-score$ of 0.99 are yielded by DarkNet19. It can be noted from Table 6, that the ACC reported by Kaur et al. [3] is very close to our proposed DarkNet19-based method. The primary advantage of the proposed model is that the proposed framework is robust and accurate as it is designed using the 10-FHCV technique, also the better error reduction is achieved by the proposed method. The limitation of the presented study is that the performance of the DLMs is tested on a single CT-scans dataset. Studying the impact of different medical images on classification accuracy is needed.

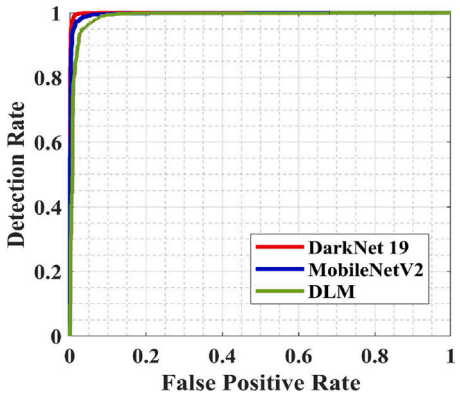

Fig. 7. Receiver operating characteristic curve plots achieved for explored DLMs.

Table 6
Performance comparison obtained for COVID-19 screening with previous methods for automated screening of COVID-19 using CT scan data.

S. No.	Authors	Classification method	Results
1.	Kaur et al. [3]	Classifier Fusion with ResNet50	ACC = 98.35% PRC = 98.02
2.	Mishra et al. [24]	Decision Fusion with DenseNet121	ACC = 88.34% $F1-score$ = 0.86
3.	Li et al. [25]	COVNet	SEN = 90.0% SPE = 96.0%
4.	Jaiswal et al. [26]	DesNet201 based DLM	ACC = 96.25% PRC = 96.29%
5.	Wang et al. [27]	Modified inceptionNet	ACC = 89.5% SEN = 87.0%
6.	Gaur et al. [30]	EWT with DenseNet121	ACC = 85.5% $F1-score$ = 0.85
7.	Soares et al. [31]	DLM	ACC = 88.6% PRC = 89.7%
8.	Goel et al. [32]	Optimized GAN	SPE = 97.78% $F1-score$ = 0.98
9.	Lu et al. [33]	CGENet	ACC = 97.78%
10.	Basu et al. [34]	Feature selection technique	ACC = 97.78% PRC = 92.88%.
11.	**Proposed Method**	**DarkNet19 with repeated holdout 10FCV**	$\mathbf{ACC}$ **= 98.91** $\mathbf{SEN}$ **= 98.96** $\mathbf{SPE}$ **= 98.86** $\mathbf{PRC}$ **= 98.88** $\mathbf{F-1score}$ **= 0.99**

6. Conclusion

CT-scan images can represent the infection caused by the COVID-19 virus in the lungs. The DLM is a powerful and useful technique to diagnose COVID-19 using CT-scan images. In this paper, an end-to-end framework is presented for the screening of COVID-19 using CT-scan images and DLMs. Two pre-trained DLMs namely, DarkNet19 and MobileNetV2 along with a newly developed less complex DLM are used in this work. The transfer learning technique is employed for benchmarked model training. A repeated 10-FHCV method is utilized to build the DLMs. Eight performance parameters are computed to measure the superiority of the proposed system. The classification results indicated that the DarkNet19 had obtained the highest classification accuracy in the classification of CT scan images into non-COVID and COVID-19 classes. The developed system may be utilized in the screening of other diseases.

CRediT authorship contribution statement

Kapil Gupta: Conceptualization, Methodology, Software, Writing – original draft, Validation. **Varun Bajaj:** Visualization, Investigation, Validation, Supervision, Writing – review & editing, Proof read.

Declaration of competing interest

The authors declare that they have no known competing financial interests or personal relationships that could have appeared to influence the work reported in this paper.

Data availability

The publicly accessible SARS-CoV-2 chest CT scan database is utilized in this work.

References

[1] U. Muhammad, M.Z. Hoque, M. Oussalah, A. Keskinarkaus, T. Seppänen, P. Sarder, SAM: Self-augmentation mechanism for COVID-19 detection using chest X-ray images, Knowl.-Based Syst. (2022) 108207.

[2] G. Bargshady, X. Zhou, P.D. Barua, R. Gururajan, Y. Li, U.R. Acharya, Application of CycleGAN and transfer learning techniques for automated detection of COVID-19 using X-ray images, Pattern Recognit. Lett. 153 (2022) 67–74.

[3] T. Kaur, T.K. Gandhi, Classifier fusion for detection of COVID-19 from CT scans, Circuits Systems Signal Process. (2022) 1–18.

[4] R.T. Gandhi, J.B. Lynch, C. Del Rio, Mild or moderate COVID-19, N. Engl. J. Med. 383 (18) (2020) 1757–1766.

[5] N. Zaki, H. Alashwal, S. Ibrahim, Association of hypertension, diabetes, stroke, cancer, kidney disease, and high-cholesterol with COVID-19 disease severity and fatality: A systematic review, Diabetes Metab. Syndr.: Clin. Res. Rev. 14 (5) (2020) 1133–1142.

[6] S.A. Harmon, T.H. Sanford, S. Xu, E.B. Turkbey, H. Roth, Z. Xu, D. Yang, A. Myronenko, V. Anderson, A. Amalou, et al., Artificial intelligence for the detection of COVID-19 pneumonia on chest CT using multinational datasets, Nature Commun. 11 (1) (2020) 1–7.

[7] S. Albahli, Efficient GAN-based chest radiographs (CXR) augmentation to diagnose coronavirus disease pneumonia, Int. J. Med. Sci. 17 (10) (2020) 1439.

[8] A. La Marca, M. Capuzzo, T. Paglia, L. Roli, T. Trenti, S.M. Nelson, Testing for SARS-CoV-2 (COVID-19): A systematic review and clinical guide to molecular and serological in-vitro diagnostic assays, Reproductive Biomed. Online 41 (3) (2020) 483–499.

[9] P. Oladimeji, J. Pickford, Letter of concern re:"Comparison of seven commercial RT-PCR diagnostic kits for COVID-19" van Kasteren et al, journal of clinical virology, J. Clin. Virol. 130 (2020) 104536.

[10] S. Woloshin, N. Patel, A.S. Kesselheim, False negative tests for SARS-CoV-2 infection—challenges and implications, N. Engl. J. Med. 383 (6) (2020) e38.

[11] I.D. Apostolopoulos, T.A. Mpesiana, COVID-19: Automatic detection from X-ray images utilizing transfer learning with convolutional neural networks, Phys. Eng. Sci. Med. 43 (2) (2020) 635–640.

[12] L. Wang, Z.Q. Lin, A. Wong, COVID-Net: A tailored deep convolutional neural network design for detection of COVID-19 cases from chest X-ray images, Sci. Rep. 10 (1) (2020) 1–12.

[13] W.H. Organization, et al., Infection Prevention and Control During Health Care When Coronavirus Disease (COVID-19) Is Suspected or Confirmed: Interim Guidance, 12 July 2021, Tech. Rep., World Health Organization, 2021.

[14] X. Xie, Z. Zhong, W. Zhao, C. Zheng, F. Wang, J. Liu, Chest CT for typical coronavirus disease 2019 (COVID-19) pneumonia: Relationship to negative RT-PCR testing, Radiology 296 (2) (2020) E41–E45.

[15] M.E. Basiri, S. Nemati, M. Abdar, S. Asadi, U.R. Acharrya, A novel fusion-based deep learning model for sentiment analysis of COVID-19 tweets, Knowl.-Based Syst. 228 (2021) 107242.

[16] S. Aydın, Deep learning classification of neuro-emotional phase domain complexity levels induced by affective video film clips, IEEE J. Biomed. Health Inf. 24 (6) (2019) 1695–1702.

[17] B. Kılıç, S. Aydın, Classification of contrasting discrete emotional states indicated by EEG based graph theoretical network measures, Neuroinformatics (2022) 1–15.

[18] S. Aydın, B. Akın, Machine learning classification of maladaptive rumination and cognitive distraction in terms of frequency specific complexity, Biomed. Signal Process. Control 77 (2022) 103740.

[19] K. Gupta, V. Bajaj, I.A. Ansari, An improved deep learning model for automated detection of BBB using ST spectrograms of smoothed VCG signal, IEEE Sens. J. 22 (9) (2022) 8830–8837.

[20] K. Gupta, V. Bajaj, I.A. Ansari, U.R. Acharya, Hyp-Net: Automated detection of hypertension using deep convolutional neural network and Gabor transform techniques with ballistocardiogram signals, Biocybern. Biomed. Eng. 42 (3) (2022) 784–796.

[21] C. Wang, X. Wang, Z. Xia, B. Ma, Y.-Q. Shi, Image description with polar harmonic Fourier moments, IEEE Trans. Circuits Syst. Video Technol. 30 (12) (2020) 4440–4452.

[22] C. Wang, B. Ma, Z. Xia, J. Li, Q. Li, Y.-Q. Shi, Stereoscopic image description with trinion fractional-order continuous orthogonal moments, IEEE Trans. Circuits Syst. Video Technol. 32 (4) (2022) 1998–2012.

[23] Z. Xia, X. Wang, W. Zhou, R. Li, C. Wang, C. Zhang, Color medical image lossless watermarking using chaotic system and accurate quaternion polar harmonic transforms, Signal Process. 157 (2019) 108–118.

[24] A.K. Mishra, S.K. Das, P. Roy, S. Bandyopadhyay, Identifying COVID19 from chest CT images: A deep convolutional neural networks based approach, J. Healthc. Eng. 2020 (2020).

[25] L. Li, L. Qin, Z. Xu, Y. Yin, X. Wang, B. Kong, J. Bai, Y. Lu, Z. Fang, Q. Song, et al., Artificial intelligence distinguishes COVID-19 from community acquired pneumonia on chest CT, Radiology (2020).

[26] A. Jaiswal, N. Gianchandani, D. Singh, V. Kumar, M. Kaur, Classification of the COVID-19 infected patients using DenseNet201 based deep transfer learning, J. Biomol. Struct. Dyn. (2020) 1–8.

[27] S. Wang, B. Kang, J. Ma, X. Zeng, M. Xiao, J. Guo, M. Cai, J. Yang, Y. Li, X. Meng, et al., A deep learning algorithm using CT images to screen for Corona virus disease (COVID-19), Eur. Radiol. (2021) 1–9.

[28] C. Li, Y. Yang, H. Liang, B. Wu, Transfer learning for establishment of recognition of COVID-19 on CT imaging using small-sized training datasets, Knowl.-Based Syst. 218 (2021) 106849.

[29] L. Sarker, M.M. Islam, T. Hannan, Z. Ahmed, COVID-DenseNet: A deep learning architecture to detect COVID-19 from chest radiology images, 2020, Preprint, 2020050151.

[30] P. Gaur, V. Malaviya, A. Gupta, G. Bhatia, R.B. Pachori, D. Sharma, COVID-19 disease identification from chest CT images using empirical wavelet transformation and transfer learning, Biomed. Signal Process. Control 71 (2022) 103076.

[31] E. Soares, P. Angelov, S. Biaso, M.H. Froes, D.K. Abe, SARS-CoV-2 CT-scan dataset: A large dataset of real patients CT scans for SARS-CoV-2 identification, 2020, MedRxiv, Cold Spring Harbor Laboratory Press.

[32] T. Goel, R. Murugan, S. Mirjalili, D.K. Chakrabartty, Automatic screening of COVID-19 using an optimized generative adversarial network, Cogn. Comput. (2021) 1–16.

[33] S.-Y. Lu, Z. Zhang, Y.-D. Zhang, S.-H. Wang, CGENet: A deep graph model for COVID-19 detection based on chest CT, Biology 11 (1) (2022) 33.

[34] A. Basu, K.H. Sheikh, E. Cuevas, R. Sarkar, COVID-19 detection from CT scans using a two-stage framework, Expert Syst. Appl. (2022) 116377.

[35] M. Sandler, A. Howard, M. Zhu, A. Zhmoginov, L.-C. Chen, Mobilenetv2: Inverted residuals and linear bottlenecks, in: Proceedings of the IEEE Conference on Computer Vision and Pattern Recognition, 2018, pp. 4510–4520.

[36] J. Redmon, A. Farhadi, YOLO9000: Better, faster, stronger, in: Proceedings of the IEEE Conference on Computer Vision and Pattern Recognition, 2017, pp. 7263–7271.

[37] J. Ma, Y. Song, X. Tian, Y. Hua, R. Zhang, J. Wu, Survey on deep learning for pulmonary medical imaging, Front. Med. 14 (4) (2020) 450–469.

[38] M. Gour, S. Jain, Automated COVID-19 detection from X-ray and CT images with stacked ensemble convolutional neural network, Biocybern. Biomed. Eng. 42 (1) (2022) 27–41.

[39] A. Dhillon, G.K. Verma, Convolutional neural network: A review of models, methodologies and applications to object detection, Prog. Artif. Intell. 9 (2) (2020) 85–112.

[40] K. Gupta, V. Bajaj, I.A. Ansari, OSACN-Net: Automated classification of sleep apnea using deep learning model and smoothed Gabor spectrograms of ECG signal, IEEE Trans. Instrum. Meas. 71 (2021) 1–9.

[41] A. Özcan, E. Dönmez, Bacterial disease detection for pepper plant by utilizing deep features acquired from DarkNet-19 CNN model, Dicle Üniversitesi Mühendislik Fakültesi Mühendislik Dergisi 12 (4) (2021) 573–579.

[42] S.J. Pan, Q. Yang, A survey on transfer learning, IEEE Trans. Knowl. Data Eng. 22 (10) (2010) 1345–1359.

[43] R. Kohavi, et al., A study of cross-validation and bootstrap for accuracy estimation and model selection, in: Ijcai, vol. 14, no. 2, Montreal, Canada, 1995, pp. 1137–1145.